Journal of Applied Polymer Science

Structure and relaxation in cellulose hydrogels

Zhiyong Xia, Marcia Patchan, Jeffrey Maranchi, Morgana Trexler
The Johns Hopkins University, Applied Physics Laboratory, Laurel, Maryland 20723
Correspondence to: Z. Xia (E-mail: Zhiyong.Xia@jhuapl.edu) and M. Trexler (E-mail: Morgana.Trexler@jhuapl.edu)

ABSTRACT: Cellulose-based hydrogels show great potential for a wide range of applications. However, the structure of these hydrated gels is not fully understood. The impact of moisture on the structure and stability of cellulose based hydrogels is reported in this article. Analytical data based on GPC, NMR, and rheology are discussed. It was found that moisture-induced gelation greatly reduces the crystallinity of the hydrogels, and the release of water from the hydrogels leads to permanent structural changes in the network structure due to the reformation of hydrogen bonding. © 2015 Wiley Periodicals, Inc. J. Appl. Polym. Sci. **2015**, *132*, 42071.

KEYWORDS: cellulose; hydrogels; relaxation

Received 9 December 2014; accepted 30 January 2015
DOI: 10.1002/app.42071

INTRODUCTION

Cellulose-based hydrogels are three dimensional (3D) network structures with a large amount of trapped water. These hydrogels have found applications in tissue engineering, controlled drug release, contact lenses, and disposable diapers applications.[1–4] Compared to chemically crosslinked hydrogels which require covalent bonding for the formation of 3D networks, cellulose-based hydrogels are formed mostly by hydrogen bonding via a self-assembly process. Formation of cellulose-based hydrogels starts by the dissolution of crystalline cellulose powder. Due to the high intrinsic crystallinity and high level of hydrogen bonding between the anhydrous glucose main chains and within the main chains (Figure 1), strong organic solvents such as *N*,*N*-dimethylacetamide (DMAc) in the presence of LiCl salt are generally used for dissolution.[5–8] The gradual dissolution of cellulose starts by the formation of hydrogen bonding between the hydroxyl protons of the anhydroglucose unit in cellulose with the Cl^- in LiCl. The Cl^- is then attracted to the $(LiDMAc)^+$ macrocation. The latter leads to the formation of repulsive forces between different segments of the host cellulose. The repulsive forces will then open more micropores, allowing more solvent to penetrate into the cellulose matrix. Due to the anhydrous nature of the above solution, the presence of moisture leads to the regeneration of hydrogen bonding between the dissolved cellulose segments, that is, gelation. Throughout this process, cellulose main chains assemble into a 3D network structure by reforming hydrogen bonds between various OH^- groups on the anhydrousglucose units. Due to the fast reaction kinetics and high hydrophilicity of the anhydrousglucose units, large amounts of moisture are trapped in the gel.

Recently, we reported the synthesis and crosslinking behavior of hydrogels based on Avicel PH101 cellulose powder (with a nominal particle size of 50 μm from FMC Biopolymer) for ocular bandage applications.[10,11] In this article, the microstructure and relaxation of these hydrogels is studied. The main focus of this work is to understand the effect of moisture on the structure of these hydrogels, which is of interest to guide incorporation of drugs into these ocular bandage gels.

EXPERIMENTAL

Hydrogel Preparation

A detailed synthesis procedure has been previously reported.[10] Briefly, Avicel 101 cellulose powder (2, 3, and 5 g) was soaked in 100 mL *N*,*N*-DMAc for 24 h followed by the addition of 8 g of LiCl. The subsequent hydrogels are referred to as 2%, 3%, and 5% samples. The solution was then heated to 95°C under agitation to form a uniform clear solution. The anhydrous solution was then poured into a silicone mold (4 mm × 3 mm × 40 mm). The mold containing the cellulose solutions was then exposed to 73% relative humidity at 35°C and left for 12 h for complete gelation. The gelled sample was then washed with deionized (DI) water at least five times to remove any excess LiCl and DMAc. Samples were then soaked in DI water before testing. Complete removal of Li^+ and DMAc was confirmed by inductively coupled plasma-optical emission spectroscopy (Varian VistaPro) and Fourier transform infrared spectroscopy (Perkin Elmer Spectrum 100), respectively.[10]

Nuclear Magnetic Resonance Analysis

To understand the 3D structure of the hydrogels, solid state ^{13}C CPMAS NMR (nuclear magnetic resonance) was performed on three representative samples: (a) as-received Avicel 101 powder,

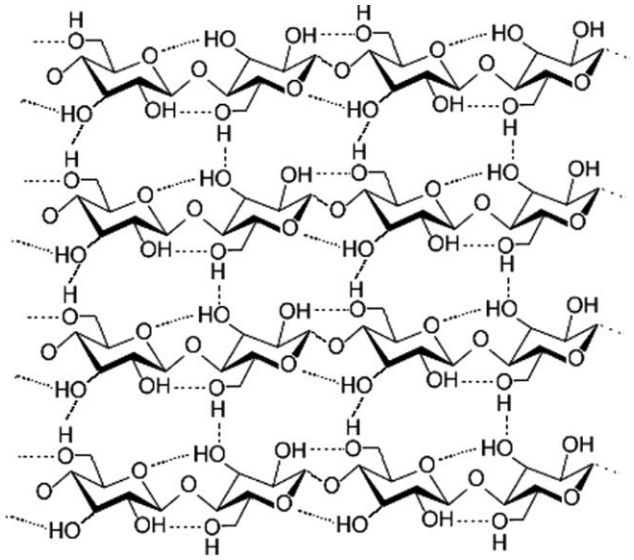

Figure 1. Structure of type I cellulose. The presence of hydrogen bonding between the main anhydrous chains and within the main chains is also shown.[9]

(b) as-synthesized 5% hydrogels (hydrated), and (c) 5% hydrogel (air dried for 24 h). ^{13}C CPMAS NMR was obtained with a 1 millisecond mix time and a 3 second delay using a 363 MHz Tecmag Redstone spectrometer operated at 91.4 MHz with a spin speed of 7 kHz.

Gel Permeation Chromatography Analysis

Molecular weight of the cellulose powder and a 5% hydrogel sample were measured using a Viscotek (Model 301) gel permeation chromatography analysis (GPC) instrument with dual-angle light scattering detection. The mobile phase for the GPC analysis was DMAc containing 0.5% LiCl. Detectors are Viscotek Triple Detector Array with RI, 7° and 90° light scattering, and differential viscometer detectors.

Small Angle X-ray Scattering Analysis

Small angle X-ray scattering (SAXS) analysis was performed at Brookhaven National Synchrotron Light Source on beamline X27C. The wavelength of the X-ray source was 1.371 Å. Prior to the analysis, the sample-to-detector distance was calibrated by silver behenate to derive a sample to detector distance of 1817 mm.

Creep and Strain Recovery Test

Creep and strain recovery of hydrogels were performed using the TA Instruments RSA-G2 solid analyzer. All samples were initially stressed at 3000 Pa and relaxed for 2500 s followed by a strain recovery test. In the strain recovery stage, all initially applied stress was fully removed, and the strain was measured as a function of recovery time.

RESULTS AND DISCUSSION

Figure 2(a) shows the ^{13}C NMR results on the three representative samples. The assignments of different carbons on the cellulose backbone and linkages between adjacent anhydroglucose units are also shown schematically in Figure 2(b). It has been well established that the different carbons in the cellulose lead to resonances at different chemical shifts (C_1: 105 ppm, C_2, C_3, C_5: 70–80 ppm, C_4: 84,89 ppm, and C_6: 63,66 ppm[12]). Among these peaks, the resonances of C_4 and C_6 are sharper and consist of broader overlapping peaks. Earl and Vanderhart[13] found that the broad wings of C_4 and C_6 correlate to the size of the crystalline phase. Recent work by Atalla and Vanderhart[14] showed that the peak at 89 ppm is due to the contribution from C_4 in the crystalline phase and the peak at 84 ppm comes from the C_4 in the amorphous phase. As a result, the crystallinity (X_c) can be computed by the finding the ratio between peak area (X) from 87–93 ppm to the total peak area ($X+Y$) from 80–93 ppm [Figure 2(a)]. That is, $X_c = X/(X+Y)$.

Using the above equation, X_c values of the three samples in Figure 2(a) are found as follows:

- Avicel 101 powder: 52%
- 5% hydrogel (hydrated): 21%
- 5% hydrogel (after air drying): 29%

The calculated 52% crystallinity in as-received Avicel 101 powder is consistent with the results reported by Park *et al.*[15] using a similar method. Compared to as-received Avicel powder, the 5% hydrogels both in hydrated and air dried states show lower crystallinity values. Two leading effects are responsible for the decrease: (1) high trapped moisture level in hydrogel, (2) formation of ether linkages between main cellulose chains through the reaction of –OH groups or hydrogen bonding during the self-assembly process. This bonding within chains in turn

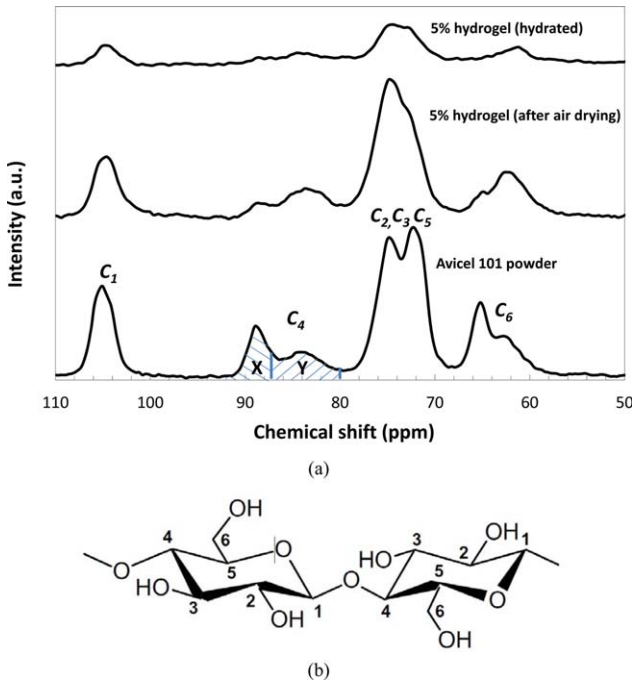

Figure 2. (a) Solid state ^{13}C NMR intensity as a function of chemical shift data for as-received Avicel 101 powder and hydrated and air dried hydrogels composed of 5% Avicel 101. The areas labeled as X and Y for the crystallinity calculation are indicated in the lower curve, (b) assignments of different carbons on the cellulose main chain. [Color figure can be viewed in the online issue, which is available at wileyonlinelibrary.com.]

Table I. Molecular Weight and Molecular Weight Distribution of Cellulose Powder and 5% Hydrogels (Hydrated) Revealed by GPC

	Cellulose powder (as-received)	5% hydrogel (hydrated)
Number average molecular weight (M_n)	16,873 ± 267	19,650 ± 388
Weight average molecular weight (M_w)	42,117 ± 822	45,408 ± 218
Molecular weight distribution (MWD)	2.56 ± 0.01	2.31 ± 0.06

disrupts the chain packing density, that is, low crystallinity. GPC results in Table I show that hydrogels have higher molecular weight than the as-received cellulose powder, indicating the formation of more intermolecular linkages in the hydrogels. Compared to the hydrated sample, crystallinity of air dried sample only has slightly higher crystallinity (29% vs. 21%). Since drying removes >90% by weight of the moisture content in the hydrogel, drying may have caused extensive reduction in the packing order of the cellulose macromolecules.

To further understand the effect of moisture level on the properties of hydrogels, hydrogels made with 2%, 3%, 5% cellulose powder were dried under ambient conditions (23°C, 30% relative humidity) for 24 h. At the end of the drying process, all hydrogels lost more than 90% (by weight) of the retained water and sample volume reduced by 80% [Figure 3(a)]. To probe the reversibility of the drying process, the dried gel sample was rehydrated in DI water at 23°C for 5 days. After the rehydration, the initial sample dimension was only slightly recovered [Figure 3(b)], which indicates that in the dried gels, some new hydrogen bonds might have reformed leading to some partial micropore closure. The latter in turn prevents water from fully re-entering into the network structure.

Based on the above analysis, it is reasonable to hypothesize that the hydrogels possess a structure shown in Figure 4. Within this structure the presence of moisture plays an important role in keeping the hydrogels hydrated. Since the water molecules are present mostly between the anhydroglucose chains, drying of hydrogels will lead to the formation of new hydrogen bonds and cause the collapse of micropores.

To investigate the aggregation state of the cellulose molecules in the hydrogels, SAXS fractal analysis was performed, and the results are shown in Figure 5, from which one can see that the structures in all three samples have complex fractal dimensions. It is generally believed that different slopes in the SAXS scattering intensity ($I(q)$) versus scattering vector ($q = 4\pi sin\theta/\lambda$, where θ is the scattering angle, and λ is the wavelength of the X-ray beam (1.37 Å)) curve correspond to different fractal structures in the scattering media:[16]

- For mass fractals (structures containing branching and cross-linking form the 3D network structure): $I(q) \sim q^{-Dm}$, and $1 < D_m < 3$, where D_m is the mass fractal dimension.
- For surface fractals (particles with fractal rough surfaces), $I(q) \sim q^{-(6-D_s)}$, and $1 < D_s < 3$, where D_s is the surface fractal dimension.

Figure 5(a) shows the $q^2I(q)$–q curves for all three representative samples, from which it can be seen that cellulose powder follows the surface fractal model with a fractal dimension $D_s = 6 - 3.55 = 2.45$. Both hydrated and air dried hydrogels follow mass fractal model with the fractal dimensions D_m of 1.96 and 1.78, respectively. The proximity of D_m for the hydrogel to 2 (versus a measured value of 1.96) indicates the presence of Gaussian chains, whereas the dried gel behaves more like swollen chains, as revealed by the proximity of D_m to 5/3.[17,18] The 2D SAXS patterns of all three samples are shown in Figure 5(b) from which no preferred orientation can be observed. Detailed analysis of the Lorentz corrected $q^2I(q)$–q curve yielded no observable long period indicating the absence of long term order.

Due to the macromolecular nature, these hydrogels are prone to stress relaxation and creep. Understanding this aspect of these

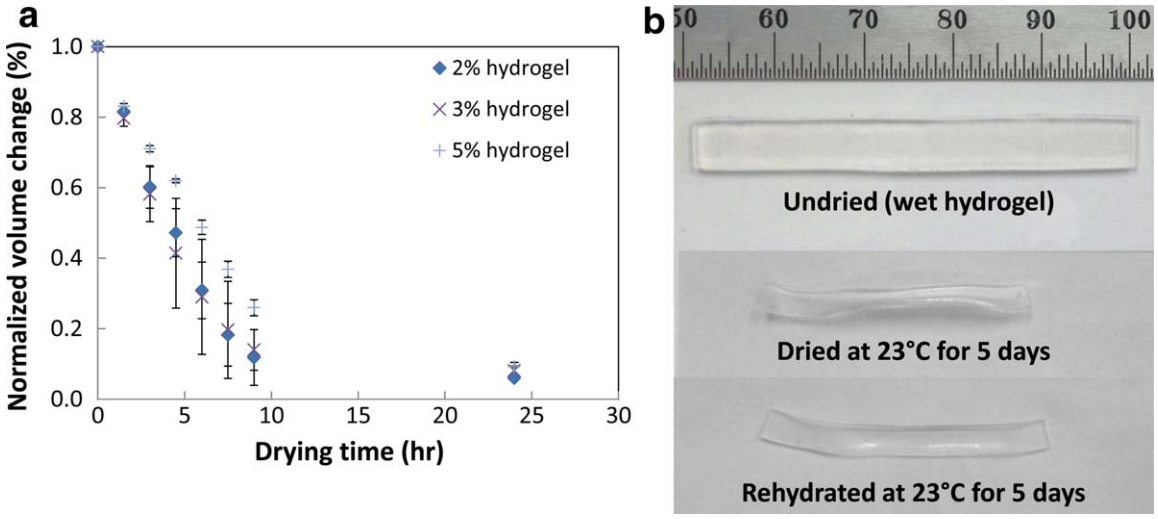

Figure 3. (a) Volume change as a function of drying time at 23°C, 30% relative humidity, (b) representative hydrogel shape change in 5% hydrogels after air drying and rehydration. [Color figure can be viewed in the online issue, which is available at wileyonlinelibrary.com.]

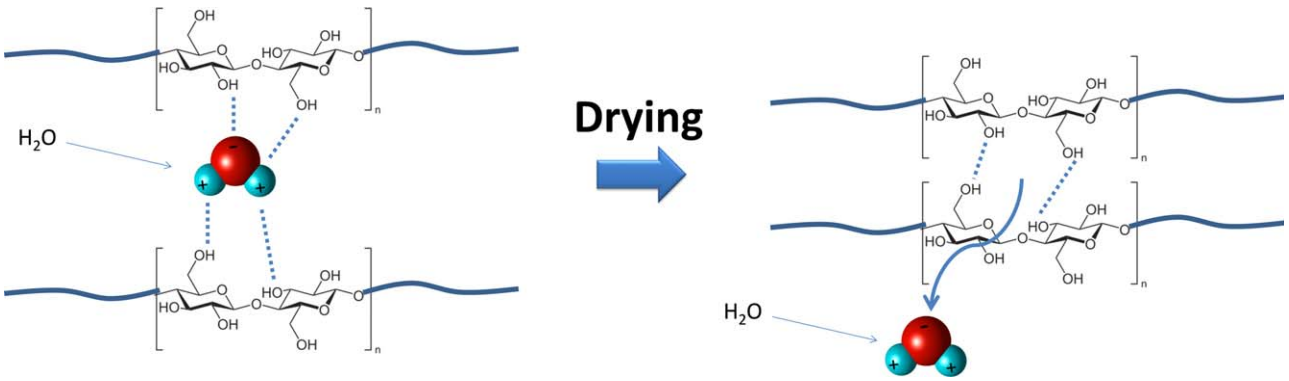

Figure 4. Schematic showing the 3D structure of hydrogel and reduction in volume following moisture removal. Dotted lines represent hydrogen bonding. [Color figure can be viewed in the online issue, which is available at wileyonlinelibrary.com.]

materials is useful for ensuring long-term stability for contact lens or ocular bandage applications. Figure 6 shows the creep and strain recovery of three hydrogels made with 2%, 3%, and 5% cellulose. All samples were initially stressed at 3000 Pa and relaxed for 2500 s followed by a strain recovery test. In the strain recovery stage, all initially applied stress was fully removed and the strain was measured as a function of recovery time.

Using the four element Maxwell-Voigt model (below), the elastic modulus (E), viscosity (η), and retardation time (λ) are obtained from curve fitting the creep and strain recovery curves in Figure 6(a).

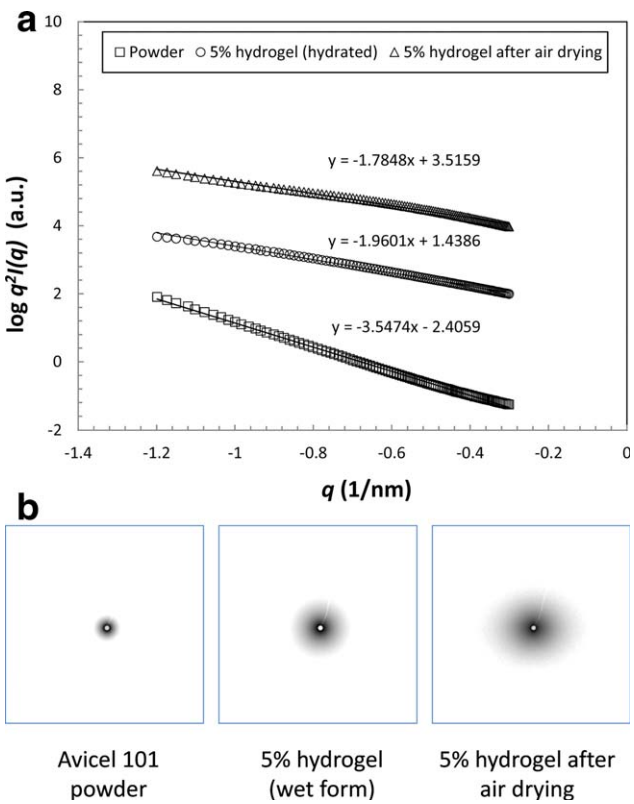

Figure 5. (a) $q^2I(q)$–q curves and (b) SAXS 2D patterns for Avicel 101 powder and 5% hydrogel (hydrated) and 5% hydrogel after air drying.

$\varepsilon(t) = \frac{\sigma_0}{E_1} + \frac{\sigma_0}{E_2}\left[1 - \exp\left(-\frac{t}{\lambda}\right)\right] + \frac{\sigma_0}{\eta_1}$, where λ is retardation time and is given by $\lambda = \eta_2/E_2$.

The results are shown in Table II. For all three samples, with the increase in cellulose content in the hydrogel, E_1 and λ both increase. This is within expectation since with an increase in cellulose content the effective crosslinking density in the hydrogels also increases.[2] The latter will lead to higher elastic modulus (E_1) and longer retardation time (λ). The decrease in η_1 indicates the decrease of the viscous feature of the hydrogels with the increase in cellulose concentration.

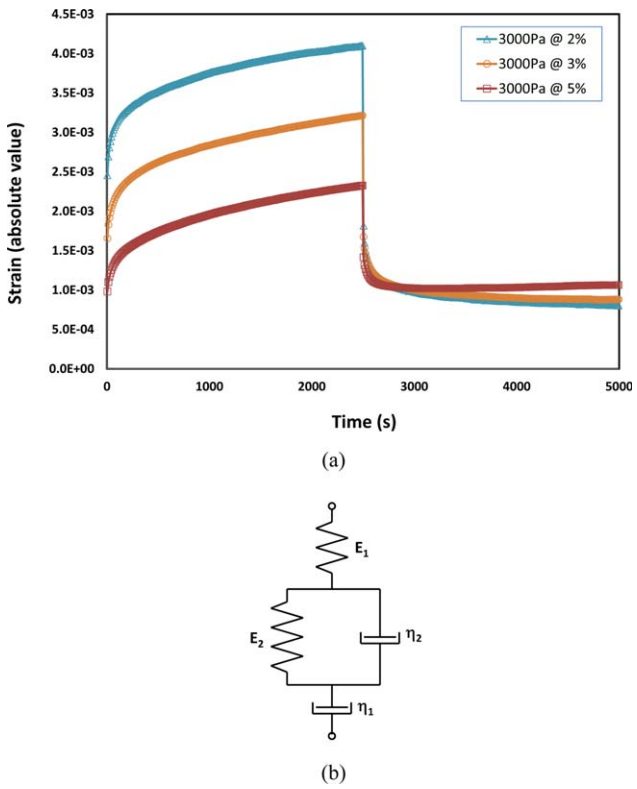

Figure 6. (a) Creep and strain recovery of three hydrogels made with different levels of cellulose. The samples were initially stressed at 3000 Pa and relaxed for 2500 s at which the stress was fully removed and strain recovery was monitored; (b) schematic of the four element Maxwell and Voigt model. [Color figure can be viewed in the online issue, which is available at wileyonlinelibrary.com.]

Table II. Characteristic Relaxation Parameters Determined Using the Four Element Model

Nominal cellulose content in hydrogel (%)	E_1 (MPa)	η_1 (GPa s)	$\lambda = \eta_2/E_2$ (retardation time) (s)
2	1.28	9.4	66
3	1.91	8.5	72
5	3.26	7.1	182

Standard deviation for E_1 is 0.01, η_1 is 0.14 and for λ is 10 s.

CONCLUSION

Based on the above analyses, it is evident that the formation of cellulose-based hydrogels and their specific structure is largely dependent on trapped moisture. These moisture molecules are predominantly attached to the anhydroglucose unit via hydrogen bonding. Removal of the water molecules causes the reformation of the hydrogen bonding between the anhydroglucose units, which is accompanied by large and unrecoverable volume reduction. Structural analyses showed that the formation of the hydrogels has reduced some of the chain regularity in the initial cellulose powders. SAXS showed the initial surface fractal model which described the cellulose powders converted to mass fractal models in the as-synthesized cellulose gels as well as the air dried gels. Increase in the cellulose content in the as-synthesized hydrogels led to the increase in retardation time, revealing that more stable structures can be achieved with higher cellulose concentrations.

ACKNOWLEDGMENTS

This research was sponsored by the US Department of the Army under the award number: W81XWH-09-2-0173. The U.S. Army Medical Research Acquisition Activity, 820 Chandler Street, Fort Detrick MD 21702-5014 is the awarding and administering acquisition office. The content of this article does not necessarily reflect the position or the policy of the Government, and no official endorsement should be inferred.

REFERENCES

1. Bajpai, A. K.; Shukla, S. K.; Bhanu, S.; Kankane, S. *Prog. Polym. Sci.* **2008**, *33*, 1088.
2. Khan, F.; Tare, R.; Richard, O.; Oreffo, R.; Bradley, M. *Angew. Chem. Int. Ed.* **2009**, *48*, 978.
3. Yasuda, H. *Macromol. Biosci.* **2006**, *6*, 121.
4. Akin, F.; Spraker, M.; Aly, R.; Leyden, J.; Raynor, W.; Landin, W. *Pediatr. Dermatol.* **2001**, *18*, 282.
5. McCormick, C. L.; Callais, P. A.; Hutchinson, B. H., Jr. *Macromolecules* **1985**, *18*, 2394.
6. Potthast, A.; Rosenau, T.; Sixta, H.; Kosma, P. *Tetrahedron Lett.* **2002**, *43*. 7757.
7. Zhang, C.; Liu, R.; Xiang, J.; Kang, H.; Liu, Z.; Huang, Y. *J. Phys. Chem. B* **2014**, *118*, 9507.
8. Ishii, D.; Tatsumi, D.; Matsumoto, T.; Murata, K.; Hayashi, H.; Yoshitani, H. *Macromol. Biosci.* **2006**, *6*, 293.
9. Moon, R. J.; Martini, A.; Nairn, J.; Simonsen, J.; Youngblood, J. *J. Chem. Soc. Rev.* **2011**, *40*, 3941.
10. Patchan, M.; Graham, J.; Xia, Z.; Maranchi, J.; McCally, R.; Schein, O.; Elisseeff, J.; Trexler, M. *Mater. Sci. Eng. C Mater. Biol. Appl.* **2013**, *33*, 3069.
11. Xia, Z.; Patchan, M.; Maranchi, J.; Elisseeff, J.; Trexler, M. *J. Appl. Polym. Sci.* **2013**, *127*, 4537.
12. Maciel, G. E.; Kolodziejski, W. L.; Bertran, M. S.; Dale, B. E. *Macromolecules* **1982**, *15*, 686.
13. Earl, W. L.; Vanderhart, D. L. *Macromolecules* **1981**, *14*, 570.
14. Atalla, R. H.; Vanderhart, D. L. *Solid State Nucl. Mag.* **1999**, *5*, 1.
15. Park, S.; Baker, J. O.; Himmel, M. E.; Parilla, P. A.; Johnson, D. K. *Biotechnol. Biofuels* **2010**, *3*, 10.
16. Schmidt, P. W. In The Fractal Approach in Heterogeneous Chemistry; Avnir, D. Ed.; J. Wiley & Sons:, New York, **1989**, *67*.
17. Bale, H. D.; Schmidt, P. W. *Phys. Rev. Lett.* **1984**, *53*, 596.
18. Teixeira, J. *J. Appl. Crystallogr.* **1988**, *21*, 781.